A Thoroughgoing Design of a Rapid-cycle Microfluidic Droplet-based PCR Device to Amplify Rare DNA Strands

M. Mollajan, S. Razavi Bazaz and A. Abouei Mehrizi[†]

Department of Life Sciences Engineering, Faculty of New Sciences and Technologies, University of Tehran, Tehran, Iran

†*Corresponding Author Email: abouei@ut.ac.ir*

ABSTRACT

DNA is a molecule and assortment of fruitful information of organisms and a wide range of viruses. Polymerase chain reaction (PCR) is a process used to amplify DNA strands in order to generate millions of them and extract the applicable information. Although conventional methods for PCR are flourishing to a certain extent, they have such major drawbacks as contamination, high material consumption, and low-speed function. By the combination of PCR devices with the microfluidic approach and integrating them with droplet generation technology, the mentioned problems can be eliminated. In this study, a novel two-step rapid-cycle droplet-based PCR (dPCR) device, considering the design of microchannel and heat transfer system, has been presented. First, numerous studies have been conducted to select the proper droplet generator for the integration of the droplet generation with the PCR device. Then, with the careful attention to the requirements of a PCR device, the geometry of different zones of the PCR device has been, meticulously, designed. In the next and last step, the heat transfer system for the designed zones of the PCR device has been planned. Afterward, results are examined carefully which indicate that in a cycle of PCR, they are not any major discrepancies between the designed dPCR and the ideal one—the one that is intended to be created.

Keywords: Droplet generation; Heat transfer system; Microfluidics; PCR device.

1. INTRODUCTION

Nowadays, microfluidics has been considered as a new technology which has manifold applications in different fields (Whitesides 2006, Foudeh, Didar *et al*. 2012, Wang, Brisk *et al*. 2016). One of the most important achievements of microfluidic approach is to perform diurnal laboratory experiments on the so-called "Lab-on-a-chip" systems—a system which has a myriad of applications in the fields of medicine and biology such as enzymatic (Hansen, Sommer *et al*. 2004) and DNA analysis (Kricka and Wilding 2003), proteomics (Pandey and Mann 2000), synthesis of nanoparticles (Salafi, Zeming *et al*. 2017), and drug delivery (Riahi, Tamayol *et al*. 2015, Stadler 2015). This evolution leads to much more speed of the experiments, more accurate results, and low reagent consumption, and by doing so, many various experiments can be carried out, simultaneously (Bartlett and Stirling 2003, Gong, Ramalingam *et al*. 2006).

Concurrent with the advent of PCR, "an experimental process for DNA amplification," by Kary Mullis (Wittwer, Reed *et al*. 1994) whose usage is in the molecular biology, a great development has occurred in the medicine field. Some of its important applications can be listed as clinical diagnosis, genetic sequencing, forensics analysis, infectious disease detection, archeology experiment, and food quality control (Zhang, Xu *et al*. 2006). PCR devices have three stages and these stages should recur so as to a DNA strand amplifies. The way that these devices work is that in each cycle, the reagent solution (DNA sample, primers, and nucleotides) is exposed to the three distinct temperature zones and after 30 to 40 cycles, DNA samples are amplified. In the first stage whose name is denaturation, the solution temperature reaches the temperature of 90ºC to 95°C, and DNA strands are separated. Then, in the second stage which is called annealing, the solution experience the circumstance at the temperature of 40ºC to 60ºC, and the primers are connected to DNA strands. In the last stage, named as extension, primers are extended their length by polymerase enzymes and new DNA strands are created (Thomas, Orozco *et al*. 2014).
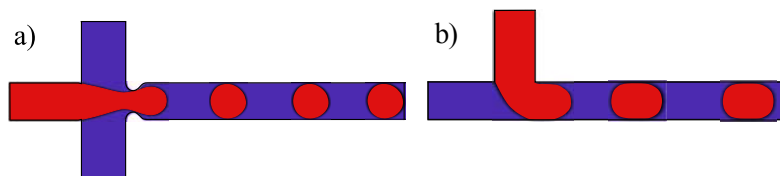
Fig. 1. Droplet generation by a) flow-focusing method and b) T-junction method.

PCR devices in macroscale have disadvantages such as the possibility of contamination when dealing with the chambers; excessive reagent consumption, especially the one which has high price or it is rare; high thermal mass; and low-speed performance. By miniaturization of these devices, as well as using microfluidic techniques, the mentioned problems can be overcome. Low reagent consumption, high heat transfer, rapid mixing of samples due to the high surface to volume ratio, and reduction of operating time are some advantages of PCR devices in microscale. Another useful and beneficial feature of these devices is the portability, and no matter where you want to carry or move your device, you can perform it, readily (Mohr, Zhang *et al*. 2007). Generally, PCR-on-a-chip devices are classified into the two different types as PCR with chambers and PCR with continuous flow (Cheng, Shoffner *et al*. 1996). In the former one, reagent solution is inside an enclosure in microscale and its temperature reaches a specified range after a number of cycles by the heating system. In the latter one, the reagent moves among three separated zones, each of which is related to a thermal area, which are elaborated before. Thermal inertia is lower in this type in comparison with the other type, because only the solution is heated. But in PCR with chambers, the whole chip should be heated to the desired temperature. Accordingly, PCR with the continuous flow is more reliable than the other one (Kopp, Mello *et al*. 1998).

In PCR with continuous flow, reagent solution moves into microchannels in single-phase, and therefore, the possibility of diffusional dilution, sample contamination, and sticking the sample to the surface exist (Kopp, Mello *et al*. 1998). As a result, if reagent solution, including DNA sample, can be transformed to the separate droplets and carried by a non-miscible fluid, those problems are avoided (Chiou, Matsudaira *et al*. 2001). By using droplet microfluidic technology, a plethora of droplets in micro- and nanoscale are generated, each of which has the aqueous solution of DNA sample and required reagents for reproduction (Thomas, Orozco *et al*. 2014). Thus, each droplet acts as a microreactor, and there is an ability to control each droplet (Chiou, Matsudaira *et al*. 2001). Additionally, the temperature distribution in each droplet is uniform, and all DNA molecules reach the desired temperature, and, as a matter of fact, the device accuracy is increased. Furthermore, the problems of sticking the sample to the surface and contamination that are associated with the PCR with continuous flow reduced significantly by using non-miscible fluid (Dak, Ebrahimi *et al*. 2016). The main conclusion to be drawn from the above description is

that droplet generation is one of the most momentous processes of designing a droplet-based PCR (dPCR). The reason behind it is that the size, the stability, and the velocity of each droplet directly affects the accuracy and the speed of the device. In order to diagnose diseases by DNA analysis more accurate and precise, it is crucial that all DNA molecules are amplified. The smaller the droplets, the more the possibility of DNA amplification. Furthermore, rare DNA samples which are not feasible to amplify by ordinary methods can be reproduced (Lee, Walker *et al*. 2009). There are some parameters that influence the size and stability of droplets such as flow rate of two solutions and surface tension between them, the contact angle between fluid and surface, physical properties of carried fluid, and geometrical parameters of droplet generators. Recently, numerous methods are used for droplet generation. T-junction and flow-focusing methods are more prevalent than others due to the production of stable and monodispersed droplets. Fig. 1 demonstrates these two methods. In the flow-focusing method, the core flow reaches the two separate shear flow in the junction which means there is a symmetrical shear force, and as a result, droplets are formed as monodispersed droplets and have a relative suitable stability, and in comparison to the T-junction method, there is a better control on each droplet. In addition, by using flow-focusing method, droplets in the order of nanometers can be produced which is not possible by T-junction method (Teh, Lin *et al*. 2008).

Another important step toward designing a PCR is the heat transfer system. Reaching the temperature of each droplet to the desirable one in each zone shows the accuracy of device (Miralles, Huerre *et al*. 2013). In PCR devices, in order to achieve the high specificity, the possibility of combination of annealing and extension zones exists (Wittwer, Herrmann *et al*. 2001). Therefore, the designed PCR has two separated zones which are denaturation (DE) (first zone) and annealing/extension (AE) zone (second zone), and a direct micro-heater is used in each zone. Furthermore, time is one of the most important parameters that affect directly the function of DNA amplification. Droplets in each cycle should be placed in each zone for a specific time. For the dPCR, the duration of each cycle should be at least 4 to 6 seconds and the relative time between two zones when droplets move among them have to be the same and 1:2 (Mohr, Zhang *et al*. 2007).

The aim of this study is to design a dPCR device, including designing a droplet generation system by a flow-focusing method, the dimensions of microchannel, and a heat transfer system. It is worth mentioning that all parameters affect the droplets are
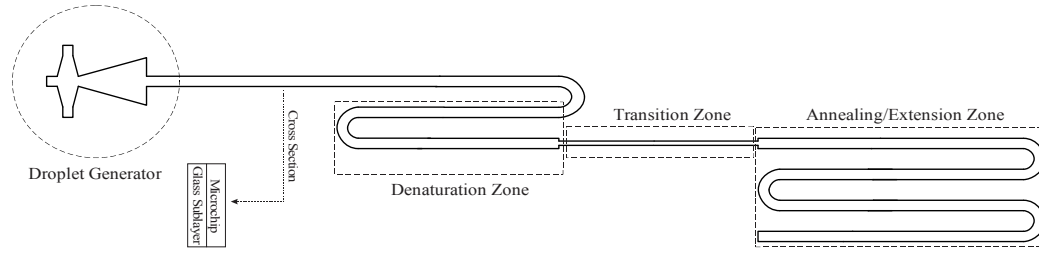
Fig. 2. The geometry design of the dPCR.

investigated meticulously. In addition, the dimensions of microchannel are designed in a way to control the relative time between two zones as well as the duration of each cycle. After that, the amount of heat that should be produced by heat transfer system in order to meet the requirements of dPCR device is calculated and applied. Then, the thermal distribution of each droplet when it moves through the microchannel is plotted, and the analogy between the designed dPCR and the ideal one in one cycle is drawn.

2. GEOMETRY DESIGN AND SIMULATION

The design of dPCR is divided into the four several parts, each of which is separately elaborated upon. At the first, the governing equations of whole system will be described. Then, in the second part, for integration of droplet generator with the PCR, the best properties of droplet generator among several studies will be selected by Taguchi method. Afterward, with punctilious attention to the requirements of a PCR, the geometry design of PCR will be chosen. Fig. 2 shows the schematic design of the dPCR. As it is shown in Fig. 2, there is a sublayer placed under the chip which is responsible for the heat transfer system. As a result, in the last part, the heat transfer system will be represented.

2.1 Governing Equations

The simulations of this study are carried out by Comsol 5.2, a commercial CFD package based on finite element method, and for this specific study, servative level set (LS) method which was introduced by Olsson and Kreiss (Olsson and Kreiss 2005) is used and shown by Eq. (1).

$$\frac{\partial \emptyset}{\partial t} + \vec{u}.\nabla\emptyset = \gamma\nabla.(\epsilon\nabla\emptyset - \emptyset(1-\emptyset)\frac{\nabla\emptyset}{|\nabla\emptyset|}) \qquad (1)$$

In Eq. (1), $\emptyset$ is the relative volume of each phase that its range is between 0 to 1, $\vec{u}$ is the velocity field, γ and ϵ are stabilization parameters that γ shows the amount of reinitialization of the level set function, and the best value of which is the maximum amount of velocity, and ϵ is a parameter regulating the thickness interface of two phases. The interfacial parameters are $\hat{n}$ and κ that can be calculated by Eqs. (2) and (3).

$$\hat{n} = \frac{\nabla\emptyset}{|\nabla\emptyset|} \qquad (2)$$

$$\kappa = -\nabla.\hat{n}|_{\emptyset=0.5} \qquad (3)$$

The surface tension between two immiscible fluids is calculated by Eq. (4) as follows.

$$\overrightarrow{F_{sf}} = \sigma\kappa\delta\hat{n} \qquad (4)$$

where σ is surface tension coefficient. While δ can be approximated by Eq. (5) (Olsson and Kreiss 2005), it is of the great importance to mention that δ equals a Dirac delta function that is nonzero only at the fluid interface.

$$\delta = 6|\nabla\emptyset||\emptyset(1-\emptyset)| \qquad (5)$$

The governing equations of the fluid in the microchannel are continuity and momentum which are described by Eqs. (6) and (7).

$$\frac{\partial\rho}{\partial t} + \nabla.(\rho\vec{u}) = 0 \qquad (6)$$

$$\rho\left(\frac{\partial u}{\partial t} + u \cdot \nabla u\right) - \nabla \cdot (\mu(\nabla u + \nabla u^T) + \nabla p = F_{sf} \qquad (7)$$

where ρ and μ are the density and viscosity, respectively. To evaluate the gravity force in the microfluidic devices, the dimensionless number of Bond (Bo) is defined by Eq. (8).

$$Bo = \frac{\Delta\rho g L^2}{\sigma} \qquad (8)$$

where $\Delta\rho$ is the difference of density between two fluids and L is characteristic length of the microchannel. Due to the fact that in microfluidic applications Bo is far lower than 1, gravity force can be ignored. Furthermore, in this study, magnetic and electric forces as well as other volumetric ones do not exist and just the surface tension appears in the momentum equation which is implemented by defining the surface tension components (Gu, Duits *et al*. 2011).

When fluids move through the microchannel, thermal energy is carried. The thermal inertia for a moving fluid has significant effect on the thermal distribution. Therefore, the energy equation can be calculated by Eq. (9).

$$\rho u b C_p \frac{\partial T}{\partial t} + \rho u c C_p.\nabla T = \nabla.(b k \nabla T) + b q'' \qquad (9)$$

where C_p is the specific heat capacity, k is the thermal conductivity coefficient, b is the width of microchannel, and q'' is the heat flux.

2.2 Design of the Flow-Focusing Droplet Generator

The flow-focusing method is used for droplet

Table 1 Values of different parameters based on the Taguchi method

Parameter	Experiments							
	No. 1	No. 2	No. 3	No. 4	No. 5	No. 6	No. 7	No. 8
V_{oil} [m/s]	0.05208	0.10416	0.05208	0.02604	0.00434	0.07812	0.02604	0.07812
V_{DNA} [m/s]	0.00434	0.00173	0.00954	0.00954	0.001302	0.00173	0.00694	0.00434
ρ_{oil} [kg/m^3]	700	1800	1500	1100	895	700	1800	1100
μ_{oil} [Pa.s]	0.002	0.041	0.041	0.028	0.02764	0.028	0.015	0.028
σ [N/m]	0.00925	0.02175	0.003	0.02175	0.0156	0.0155	0.002175	0.00925

generation which produces droplets by shear flow. This method which was first employed by Anna *et al.* (Anna, Bontoux *et al.* 2003) is mainly applied for generation of small droplets with high efficiency. In the flow-focusing method, two immiscible fluids flow together in a centered manner so that the continuous phase flows on the both sides of the shear phase. With decreasing the width of microchannel, two fluids compressed simultaneously, and the flow field generated by this condition leads to the formation of a jet in the shear flow, and finally, it produces droplets (Christopher and Anna 2007). Capillary number plays a significant role in formation of droplets in microfluidic devices. Eq. (10) represents this dimensionless number (Glawdel 2012).

$$Ca = \frac{\mu u}{\sigma} \tag{10}$$

where it demonstrates the ratio of viscous force to the surface tension. Surface tension leads to change the interfacial area which is an important parameter in generation and stability of droplets. In Capillary number of less than 1, the surface tension is dominant and spherical droplets are produced, whereas in Capillary number more than 1, viscous force is dominant and asymmetrical droplets are formed. In flow-focusing method, droplets have a diameter less than the dimensions of the orifice. Also, the diameter of droplets decreases by decreasing the relative flow rates and Capillary number. In low Capillary numbers, the formation of droplets occurs by dripping and by increasing Capillary number, a transition mode between dripping and jetting happens. When the droplet generation occurs by jetting, droplets have a big relative diameter with non-uniform shape. In order to generate stable and monodispersed droplets by the flow-focusing method, the droplet generator that is illustrated in Fig. 3, which was adapted from Tan *et al.* (Tan, Cristini *et al.* 2006) has been used. Due to the fact that the extracted DNA is in an aqueous diluted water solution, the thermal and physical properties of the DNA solution are assumed to be the same as the water. (Eslamian and Saghir 2012, Kumar, Cartas-Ayala *et al.* 2013, Thomas, Orozco *et al.* 2014) and water is used as the main flow which is inserted from straight inlet, and oil is used as the shear flow which is inserted from side inlets. Numerous parameters affect the stability and dimensions of the droplets (Lashkaripour *et al.* 2015). In order to find out the best droplet generator in which the droplets are stable and monodispersed, a series of experiments, all of which are shown in

Table 1, are designed. In each experiment, the angle of fluid and wall is assumed as $3\pi/2$. Due to the limitations of fabrication and the problem of sticking a sample to the surface of wall, the relation between the surface to volume of the microchannel should not be high enough.

Table 2 shows the mesh study of the droplet generation part of paper. The nominated grid, c, is illustrated in Fig. 3.

Table 2 Grid study with different mesh elements for the droplet generation section

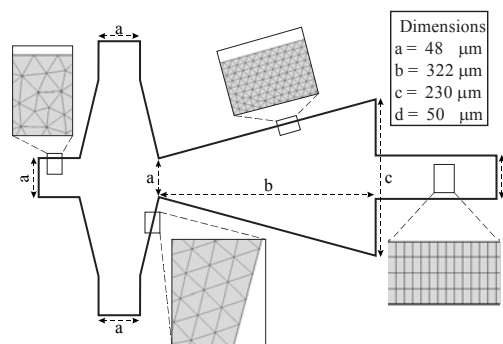| Mesh	Number of elements	V_{out} [m/s]	Error
a	1004	0.0294	----
b	1686	0.0266	0.0952
c	2658	0.0257	0.035
d	11582	0.0251	0.023

Fig. 3. The geometry design of droplet generator, which is a part of the designed dPCR and was adapted from Tan *et al.* (Tan, Cristini *et al.* 2006), and mesh distribution along the length of microchannel.

Table 3 designed parameters of the microchannel

Zone	l [μm]	b [μm]	δ [μm]
Denaturation	8000	50	150
Annealing/Extension	8000	50	150
Transition	4000	21.5	50

2.3 Design of the Microchannel Geometry

After the design of droplet generator, the design of the geometry of microchannel has been begun. In order to design an effective geometry, a comprehensive and

Table 4 The amount of coefficient used for the heat transfer system

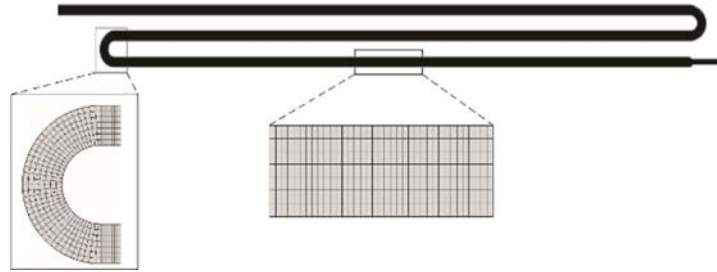| Material	C_p [J.K^{-1}.kg^{-1}]	Specific heat capacity	K [W.m^{-1}.K^{-1}]	h [W.m^{-2}.K^{-1}]	α_i [K^{-1}]
Oil	4126.1	2.046	0.17	----	----
PDMS	----	1.46	0.15	----	9.34×10^{-8}
Air	----	----	----	10	----
Glass	----	----	1.38	----	7.81×10^{-7}

Fig. 4. Mesh distribution in the curved and straight part of DE zone for the heat transfer section.

accurate understanding of the PCR device is required. The remaining time of the droplets in each zone of the dPCR is the most important criteria in designing a microchannel. The remaining time of DE zone is less than that of AE one, and for better performance, the relation between them should be 1:2. The mentioned remaining time is calculated by Eq. (11) (Kumar, Cartas-Ayala *et al.* 2013).

$$t_i = \frac{l_i b_i \delta_i}{Q} \qquad (11)$$

where i is related to each zone (DE and AE); l, b, and δ are the length, the width, and the depth of the microchannel, respectively; and Q is the volumetric flow rate of fluid. The designed parameters to satisfy the best performance based on Eq. (11) are shown in Table 3.

In order to reduce the transition time and increase the heat transfer rate between the main zones, a transition zone between DE and AE zone is designed. According to Table 3, the width of the transition zone is smaller than that of other zones. The average velocity in the each zone of microchannel can be calculated by Eq. (12) (Kumar, Cartas-Ayala *et al.* 2013).

$$V_{avg} = \frac{Q}{b\delta} \qquad (12)$$

Based on Table 3 and Eq. (12), the ratio of average velocity between DE and transition zone is 3.5. The schematic design of dPCR was illustrated in Fig. 2.

2.4 Heat Transfer System

By considering the heat flux, $q''(x)$, in the flow direction, the effect of heat transfer and thermal distribution along the length of microchannel can be extracted. The relation between the size of droplets to the carried fluid is significantly small, and also, the heat transfer coefficient of water and oil are similar to each other; therefore, droplets are neglected in this part. Additionally, the width of the microchannel is small enough to do not consider

conduction in the Y direction. The material of microchannel is considered to be PDMS, and for the glass sublayer, which was shown in Fig. 2, the coefficient of α_i as the heat loss factor is considered. The energy equation in a control volume with the length of Δx can be calculated by Eq. (13).

$$A_i \rho_f V_{avg} Cp_f \frac{dT}{dx} - A_i K_f \frac{d^2T}{dx^2} + h(x)(T(x) - T_\infty) = q''_i(x)(1 - \alpha_i)b \qquad (13)$$

where $T(x)$ is the temperature of fluid along the fluid path, and A_i is the cross section of microchannel in each location. The proper amounts of the coefficients for each material are listed in Table 4.

One aspect of this study is to obtain the required amount of heat that has to be applied by heaters to gain suitable temperature distribution in each zone. The ideal dPCR is the one that has uniform temperature distribution of 95ºC and 68ºC in the DE and AE zone in each cycle (Kumar, Cartas-Ayala *et al.* 2013). Hence, three different experiments based on Table 5 are undertaken to find the proper one for the designed dPCR device in order to be consistent with the ideal one.

Table 5 The heat flux of three different experiments

Experiment	q''_{DE} [W/m^3]	q''_{AE} [W/m^3]
1	35×10^7	13×10^7
2	85×10^7	63×10^7
3	65×10^7	43×10^7

The mesh study of heat transfer system is shown in Table 6. Fig. 4 shows the selected mesh of the simulation for DE zone. Due to the dimensional problem and because of the fact that mesh distribution of DE zone is the same as AE one, the mesh distribution of AE zone is not represented.
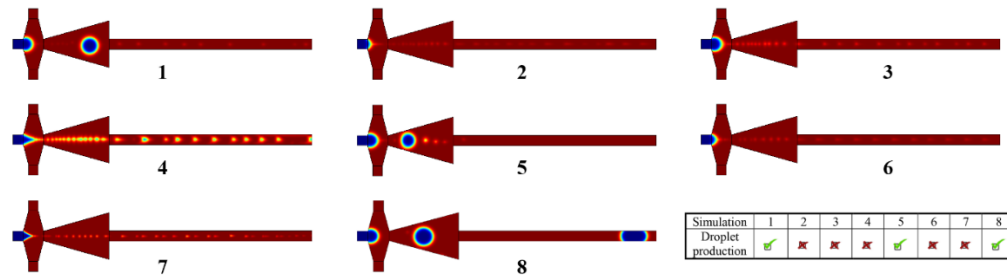
Fig. 5. Illustration of the simulation of eight experiments as well as their qualitative results.
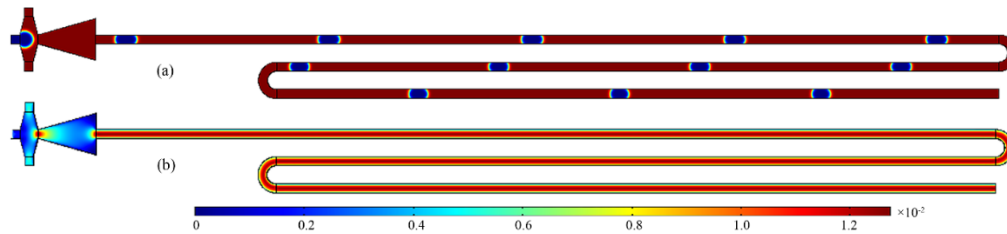

Fig. 6. (a) Generation and movement of droplets in DE zone and (b) velocity profile of the solution in the microchannel at 3rd second.

Table 6 Grid study with different mesh elements for the heat transfer section

Mesh	No. of elements	V_{out} [m/s]	Error
a	3720	0.00301	----
b	7440	0.00374	0.242
c	13900	0.00428	0.144
d	26040	0.00452	0.05

3. RESULTS AND DISCUSSION

3.1 Droplet Generation by Flow-Focusing Method

The main aim of this part is to analyze effects of different parameters on the droplet generation. The results of the experiments, which were designed in section 2.2, are demonstrated in Fig. 5. For droplet generation simulations, the level set method is applied. This method is applicable for immiscible two-phase fluids and uses the track of interface between two phases. In this part, Eqs. (1), (6), and (7) are solved simultaneously to determine the interface. These equations are time-dependent because the location of interface always depends on the previous time step.

In 1st experiment of Fig. 5, the diameter of droplets is 72 μm. 2nd, 3rd, 4th, 6th, and 7th experiments do not produce any droplet, or the diameter of them is small enough that is not suitable for the dPCR. The diameter of droplets in 5th experiment is 58 μm, and droplets move toward the center of the microchannel with a relative suitable stability. In 8th experiment, the droplet diameter is 83 μm. Droplets in 5th experiment have the least diameter and the best stability in comparison to others. In addition, the generation time of droplets in 5th experiment is 0.32 seconds, approximately, which is completely

appropriate for the dPCR. Thus, the droplet generator with the properties 5th one which were shown in Table 1 is selected for the corresponding dPCR.

3.2 Droplets Movement Along the Length of Microchannel

The geometry design of PCR was shown in Fig. 2. Fig. 6 represents the generation and movement of droplets in DE zone as well as the velocity profile of the fluid at 3rd second.

As it is obvious in Fig. 6a, all droplets move along the microchannel in a steady and monodispersed manner. Furthermore, the time that a droplet passes DE zone is about 2.18 seconds which is completely satisfactory for the rapid-cycle dPCR. Accordingly, the geometrical parameters of microchannel and droplet generation have been, accurately, designed. Based on the Fig. 6b, the velocity profile of the microchannel at 3rd second shows that the average velocity of fluid in the microchannel in DE zone is 0.0041 m/s and it is approximately same as the oil velocity. The reason behind this fact is that droplets are carried by the shear flow, and therefore, they should have the same velocity as the shear flow. According to the uniformity of the fluid velocity in DE zone, it is assumed that the time that a droplet passes among AE zone is twice of the time in DE zone, and the huge and time-consuming calculation of AE zone is, wisely, avoided.

3.3 Heat Transfer in One Cycle of dPCR

At this stage, the temperature distribution along the length of microchannel and the amount of heat that heaters should produce are obtained. Therefore, first of all, simulations are carried out, and then, the temperature distribution of different zones of dPCR is calculated. The time that a droplet passes through DE and AE zone is about 2.18 and 4.36 seconds,

respectively. As a result, the overall simulation time is assumed to be 7 seconds. The results of the three mentioned simulations which were listed in Table 5 are illustrated in Fig. 7.

Fig. **7** shows the temperature distribution of a droplet that passes through the microchannel for the three mentioned simulations. Fig. 7a shows that T_{DE} and T_{AE} will be 335 and 317K, respectively, which are less than the ideal temperatures. The results of the second experiment are shown in Fig. 7b, and T_{DE} and T_{AE} are 382 and 365K, respectively. These temperatures are above the desired one. Eventually, for the last one, as Fig. 7c also elucidates it, T_{DE} and T_{AE} will be 368 and 341 K, respectively. These temperatures completely satisfy the requirements of designed dPCR. The brief results of Fig. 7 are shown in Table 7.
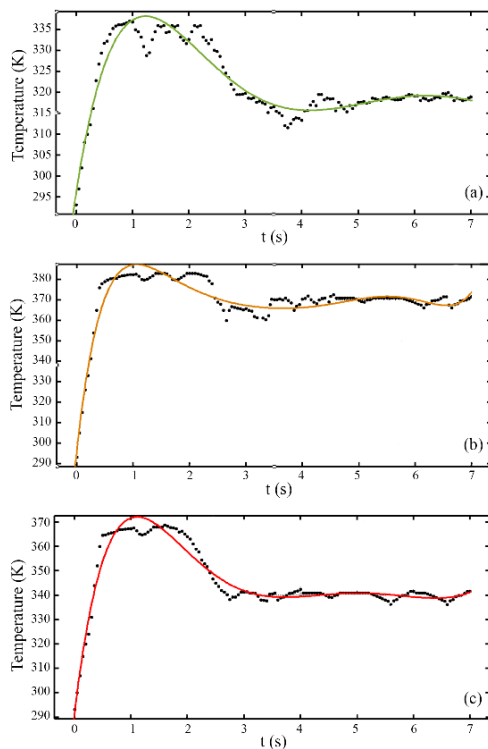

Fig. 7 The temperature distribution of three separate simulations.

Table 7 Results of the three designed simulations to obtain the appropriate thermal distribution

Experiment	Heat flux [W/m³]		Results [K]	
	$q_{DE}^{"}$	$q_{AE}^{"}$	T_{DE}	T_{AE}
1	35×10^7	13×10^7	335	317
2	85×10^7	63×10^7	382	368
3	65×10^7	43×10^7	368	341

According to 3rd experiment, which is appropriate for the designed dPCR, heat transfer rate for the transition zone—the zone between DE and AE zone—should be evaluated. Therefore, Fig. 8a shows the temperature distribution in the range of 2 to 2.7

seconds which is the time that a droplet goes from the end of DE zone to reach the inlet of AE zone. In addition, the temperature distribution of the dPCR in the different zones is represented in Fig. 8b.
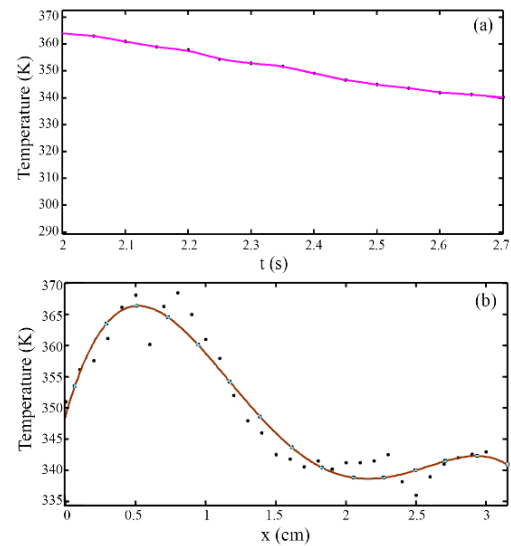

Fig. 8. a) Temperature distribution in the transition zone and b) temperature distribution in the different zones of dPCR.

Based on Fig. 8a, the temperature variation is -13 K, and as a result, the cooling rate can be calculated as 18.57 K/s which is suitable for the designed dPCR and leads to increase its performance. Likewise, Fig. 8b shows that total length of DE and AE zone are 0.7 and 1.5 cm, respectively.

3.4 Comparison of the dPCR with the Ideal One

Generally, two criteria exist to evaluate a PCR device. The first one is to obey that the relative time between DE to AE zone be 1:2. As it was investigated in section 2.3, the microchannel dimensions have been designed in a way to satisfy this demand. As a result, there is not any problem for the first criteria. The second one is that the temperature of droplets in each zone should be reached the ideal temperature. To evaluate this, there is no need to perform experimental results, and generally, the temperature diagram of droplets in the designed PCR is compared with the ideal one (Mohr, Zhang *et al*. 2007, Kumar, Cartas-Ayala *et al*. 2013, Thomas, Orozco *et al*. 2014). In order to obtain the temperature of droplets along the length of the microchannel, Lagrangian method is applied and the temperature of droplet in each time and location is extracted by this method. A comparison between the designed dPCR and the ideal one in one cycle is carried out, and the results are illustrated in Fig. 9a. In addition, the temperature difference between these two PCR devices is shown in Fig. 9b.

According to Fig. 9a, there is a difference between the designed and ideal dPCR in DE zone, and the reason why this happened is based on the fact that DE zone is a two-part zone which is connected by a

curved microchannel that leads to a small deviation from the ideal one. The transition zone roughly reduces the cooling rate between two main zones, and in AE zone, there is not any significant discrepancy in these two PCR devices. Based on Fig. 9b, due to the lack of the preheat zone in this simulation, the highest amount of error is in range of 0 to 0.6 seconds, and after that, there is not any major disagreement between them.
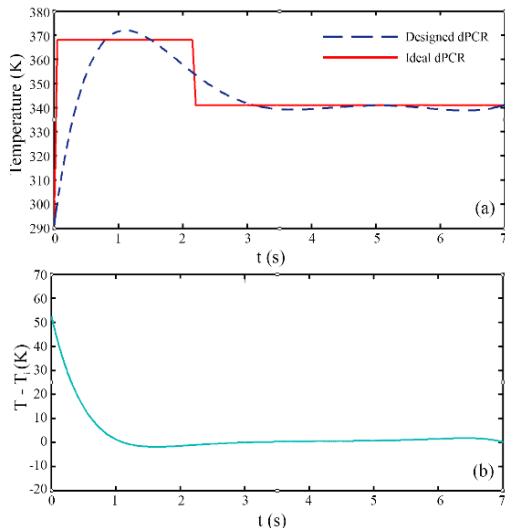

Fig. 9. a) The temperature comparison of the designed PCR and the ideal one and b) the temperature difference between these two devices.

The error between these two devices can be calculated by Eq. (14):

$$error = \left(\frac{T_i - T_s}{T_i}\right) \qquad (14)$$

The calculated error is 1.667 % which shows that the designed dPCR is in a good agreement with the ideal one. As it is investigated, the designed PCR agrees with the two mentioned criteria.

4. CONCLUSION

PCR devices are an indispensable part of clinical experiments and laboratories. Since an accurate and reliable dPCR device is always the missing link in laboratories, the aim of this study is to apply the microfluidic approach for designing a PCR device which is integrated with the droplet generator and make as a whole a dPCR device. Several distinct droplet generators have been tested to detect the best one that can produce monodispersed and stable droplets. After careful evaluations, droplet generator with V_{oil}= 0.00434 m/s, V_{DNA}= 0.001304 m/s, ρ_{oil}= 895 kg/m^3, μ_{oil}= 0.02764 Pa.s, and σ= 0.0156 N/m is selected. In order to obey the role of an ideal dPCR in one cycle in terms of temperature distribution, the geometry of microchannel in different zones (DE and AE) has been designed with punctilious attention to the protocol. The transition zone between the two stages of the dPCR has been created to increase the heat transfer efficiency. Furthermore, in order to assign an appropriate heat transfer system, many studies have been designed to find the efficient number of heat flux in different zones. The results show that the heat flux of 65×10^7 W/m^3 and 43×10^7 W/m^3 are completely proper to be applied to DE and AE zone. The temperature difference between the designed dPCR and the ideal one in one cycle shows that there is not any major divergence between them and the analogy between them is promising. Since PCR devices are ubiquitous in all laboratories, the mentioned dPCR which was design step by step with the most accuracy can satisfy all demands of biologists, and it is completely appropriate for future usage.

REFERENCES

Anna, S. L., N. Bontoux and H. A. Stone (2003). Formation of dispersions using flow focusing in microchannels. Applied physics letters 82(3), 364-366.

Bartlett, J. M. and D. Stirling (2003). A short history of the polymerase chain reaction. PCR protocols 3-6.

Cheng, J., M. A. Shoffner, G. E. Hvichia, L. J. Kricka and P. Wilding (1996). Chip PCR. II. Investigation of different PCR amplification systems in microfabricated silicon-glass chips. Nucleic Acids Research 24(2), 380-385.

Chiou, J., P. Matsudaira, A. Sonin and D. Ehrlich (2001). A Closed-Cycle Capillary Polymerase Chain Reaction Machine. Analytical Chemistry 73(9), 2018-2021.

Christopher, G. F. and S. L. Anna (2007). Microfluidic methods for generating continuous droplet streams. Journal of Physics D: Applied Physics 40(19), R319.

Dak, P., A. Ebrahimi, V. Swaminathan, C. Duarte-Guevara, R. Bashir and M. A. Alam (2016). Droplet-based Biosensing for Lab-on-a-Chip, Open Microfluidics Platforms. Biosensors 6(2): 14.

Eslamian, M. and M. Z. Saghir (2012). Modeling of DNA thermophoresis in dilute solutions using the non-equilibrium thermodynamics approach. Journal of Non-Equilibrium Thermodynamics 37(1), 63-76.

Foudeh, A. M., T. F. Didar, T. Veres and M. Tabrizian (2012). Microfluidic designs and techniques using lab-on-a-chip devices for pathogen detection for point-of-care diagnostics. Lab on a Chip 12(18), 3249-3266.

Glawdel, T. (2012). Droplet Production and Transport in Microfluidic Networks with Pressure Driven Flow Control.

Gong, H., N. Ramalingam, L. Chen, J. Che, Q. Wang, Y. Wang, X. Yang, P. H. E. Yap and C. H. Neo (2006). Microfluidic handling of PCR solution and DNA amplification on a reaction chamber array biochip. Biomedical microdevices 8(2), 167-176.

Gu, H., M. H. Duits and F. Mugele (2011). Droplets formation and merging in two-phase flow microfluidics. International journal of molecular sciences 12(4), 2572-2597.

Hansen, C. L., M. O. Sommer and S. R. Quake (2004). Systematic investigation of protein phase behavior with a microfluidic formulator. Proceedings of the National Academy of Sciences of the United States of America 101(40), 14431-14436.

Kopp, M. U., A. J. Mello and A. Manz (1998). Chemical amplification: continuous-flow PCR on a chip. Science 280(5366), 1046-1048.

Kricka, L. and P. Wilding (2003). Microchip pcr. Analytical and Bioanalytical Chemistry 377(5), 820-825.

Kumar, S., M. A. Cartas-Ayala and T. Thorsen (2013). Thermal modeling and design analysis of a continuous flow microfluidic chip. International Journal of Thermal Sciences 67, 72-86.

Lashkaripour, A., A. Abouei Mehrizi, M. Rasouli and M. Goharimanesh (2015). Numerical Study of Droplet Generation Process in a Microfluidic Flow Focusing. Journal of Computational Applied Mechanics 46(2), 167-175.

Lee, W., L. M. Walker and S. L. Anna (2009). Role of geometry and fluid properties in droplet and thread formation processes in planar flow focusing. Physics of Fluids 21(3), 032103.

Miralles, V., A. Huerre, F. Malloggi and M. C. Jullien (2013). A Review of Heating and Temperature Control in Microfluidic Systems: Techniques and Applications. Diagnostics 3(1), 33.

Mohr, S., Y.-H. Zhang, A. MacAskill, P. Day, R. W. Barber, N. Goddard, D. Emerson and P. Fielden (2007). Numerical and experimental study of a droplet-based PCR chip. Microfluidics and Nanofluidics 3(5), 611-621.

Olsson, E. and G. Kreiss (2005). A conservative level set method for two phase flow. Journal of computational physics 210(1), 225-246.

Pandey, A. and M. Mann (2000). Proteomics to study genes and genomes. Nature 405(6788), 837-846.

Riahi, R., A. Tamayol, S. A. M. Shaegh, A. M. Ghaemmaghami, M. R. Dokmeci and A. Khademhosseini (2015). Microfluidics for advanced drug delivery systems. Current Opinion in Chemical Engineering 7, 101-112.

Salafi, T., K. K. Zeming and Y. Zhang (2017). Advancements in microfluidics for nanoparticle separation. Lab on a Chip 17(1), 11-33.

Stadler, B. (2015). Preface to Special Topic: Microfluidics in Drug Delivery, AIP Publishing.

Tan, Y.-C., V. Cristini and A. P. Lee (2006). Monodispersed microfluidic droplet generation by shear focusing microfluidic device. Sensors and Actuators B: Chemical 114(1), 350-356.

Teh, S.-Y., R. Lin, L. H. Hung and A. P. Lee (2008). Droplet microfluidics. Lab on a Chip 8(2), 198-220.

Thomas, S., R. L. Orozco and T. Ameel (2014). "Thermal gradient continuous-flow PCR: a guide to design." Microfluidics and nanofluidics 17(6), 1039-1051.

Wang, J., P. Brisk and W. H. Grover (2016). Random design of microfluidics. Lab on a Chip 16(21), 4212-4219.

Whitesides, G. M. (2006). The origins and the future of microfluidics. Nature 442(7101), 368-373.

Wittwer, C. T., M. G. Herrmann, C. N. Gundry and K. S. Elenitoba-Johnson (2001). Real-time multiplex PCR assays. Methods 25(4), 430-442.

Wittwer, C., G. Reed and K. Ririe (1994). The polymerase chain reaction, ed. KB Mullis, F. Ferré and RA Gibbs, Birkhauser, Boston.

Zhang, C., J. Xu, W. Ma and W. Zheng (2006). PCR microfluidic devices for DNA amplification. Biotechnology advances 24(3), 243-284.